

# Electrodeposition of Graphitic Carbon Nitride and its Composites for Tailored Electrocatalytic Activity



Thesis submitted in partial fulfillment for the  
Award of Degree

**Doctor of Philosophy**

By

*Ankush Kumar Singh*

DEPARTMENT OF CHEMISTRY  
INDIAN INSTITUTE OF TECHNOLOGY  
(BANARAS HINDU UNIVERSITY)  
VARANASI-221005  
INDIA

**Roll No. 21051009**

**Year 2024**



**Copyright ©  
Department of Chemistry  
Indian Institute of Technology  
(Banaras Hindu University) Varanasi  
221005, India  
2024  
All rights reserved.**




# **Dedicated to my Mother**



## CERTIFICATE

It is certified that the work contained in the thesis titled “**Electrodeposition of Graphitic Carbon Nitride and its Composites for Tailored Electrocatalytic Activity**” by **Ankush Kumar Singh** has been carried out under my supervision and this work has not been submitted elsewhere for a degree.

It is further certified that the student has fulfilled all the requirements of Comprehensive Examination, Candidacy, and SOTA for the award of Ph.D. Degree.



DR. ROSY  
ASSISTANT PROFESSOR  
DEPARTMENT OF CHEMISTRY  
IIT (BHU), VARANASI

### **Signature of the Supervisor**

Dr. Rosy  
Assistant Professor  
Department of Chemistry,  
Indian Institute of Technology  
(Banaras Hindu University),  
Varanasi–221005



## DECLARATION BY THE CANDIDATE

I, “**Ankush Kumar Singh**”, certify that the work embodied in this thesis is my own bonafide work and carried out by me under the supervision of “**Dr. Rosy**” from “**July-2021**” to “**November-2024**,” at the **Department of Chemistry, Indian Institute of Technology (BHU) Varanasi**. The matter embodied in this thesis has not been submitted for the award of any other degree/diploma. I declare that I have faithfully acknowledged and given credits to the research workers wherever their works have been cited in my work in this thesis. I further declare that I have not wilfully copied any other's work, paragraphs, text, data, results, etc., reported in journals, books, magazines, reports, dissertations, theses, etc., or available at websites and have not included them in this thesis and have not cited as my own work.

**Date:** 05/11/2024


**Place:** Varanasi



(Ankush Kumar Singh)

## CERTIFICATE BY THE SUPERVISOR

It is certified that the above statement made by the student is correct to the best of my knowledge.



**DR. ROSY**  
ASSISTANT PROFESSOR  
DEPARTMENT OF CHEMISTRY  
IIT (BHU), VARANASI

**Supervisor**  
(Dr. Rosy)



Signature of Head of Department  
विभागाध्यक्ष / HEAD  
रसायन विज्ञान विभाग  
Department of Chemistry  
भारतीय प्रौद्योगिकी संस्थान (का.हि.वि.वि.)  
Indian Institute of Technology (B.H.U.)  
वाराणसी-221005 / Varanasi-221005



## COPYRIGHT TRANSFER CERTIFICATE

**Title of the Thesis:** *Electrodeposition of Graphitic Carbon Nitride and its Composites for Tailored Electrocatalytic Activity*

**Name of the Student:** *Ankush Kumar Singh*

### Copyright Transfer

The undersigned hereby assigns to the Indian Institute of Technology (Banaras Hindu University) Varanasi all rights under copyright that may exist in and for the above thesis submitted for the award of the "**Doctor of Philosophy**" degree.

**Date:** 05/11/2024



**Place:** Varanasi.

(Ankush Kumar Singh)

**Note:** *However, the author may reproduce or authorize others to reproduce material extracted verbatim from the thesis or derivative of the thesis for author's personal use provided that the source and the Institute's copyright notice are indicated.*



---

---

## ACKNOWLEDGEMENTS

---

---

I wish to extend my sincere appreciation and heartfelt thanks to all those around me whose invaluable advice, constructive criticism, unwavering support, and encouragement have made this journey possible. Their commitment and belief in my work have been a constant source of strength, and I am deeply grateful for their presence and contributions along the way.

First and foremost, it is my profound privilege to express my deepest gratitude to my esteemed supervisor, **Dr. Rosy** of the Department of Chemistry at the IIT(BHU) Varanasi. Her invaluable guidance, unwavering support, and expert insight have been instrumental in the successful completion of my research work. Her dedication to academic excellence and her passion for research have inspired and shaped me profoundly throughout this journey.

From the outset of this research to its culmination, she has consistently provided not only intellectual support but also personal encouragement and compassionate mentorship. Her insightful feedback and constructive criticism pushed me to refine my ideas, to persevere through challenging phases, and to strive for the highest standards of academic rigor. I am immensely grateful for the time and energy she devoted to every aspect of my work, often going above and beyond to ensure I could meet my goals.

Furthermore, her sustained interest in my progress and her belief in my potential have been a source of motivation and reassurance. She has been more than a supervisor; her nurturing approach provided a foundation of strength and encouragement, particularly during difficult moments, for which I am sincerely thankful. Her parental care and

thoughtful guidance created an environment in which I could thrive, and I am certain that my research journey would not have been as rewarding or fruitful without her enduring support.

In closing, I extend my deepest respect and gratitude to Dr. Rosy for all she has contributed to my personal and academic growth. Her influence will remain a guiding force as I move forward in my professional endeavours, and I am truly fortunate to have had the privilege of working under her mentorship.

I would like to extend my sincere gratitude to the former Heads of the Department of Chemistry, IIT(BHU) Varanasi, **Prof. Dhanesh Tiwari** and **Prof. Yogesh Chandra Sharma**, as well as the current Head, **Prof. Sundaram Singh**. I am deeply thankful to them, along with all the esteemed faculty members of the department, for their generous support and for providing all the necessary resources and facilities that enabled me to conduct my research with ease and efficiency. I would also like to thank the non-teaching staff of the department who were always cordial throughout this journey.

I am sincerely grateful to my RPEC members, **Prof. Dhanesh Tiwari** from the Department of Chemistry and **Dr. Prodyut Dhar** from the School of Biochemical Engineering at IIT(BHU) Varanasi. Their valuable suggestions, steady guidance, and encouraging support have greatly enriched my research experience and contributed significantly to my progress.

I am grateful to our collaborators, **Aarti Saroj** and **Dr. V. Ramanathan** from the Department of Chemistry, IIT(BHU) Varanasi for their assistance with Raman analysis.

I also thank **Hemanth** and **Dr. Udit Ghosh** from the Department of Chemical

Engineering for their support with the microscopic analysis of drop-casted gCN. Their contributions have been invaluable to the progress of my research.

I gratefully acknowledge the **Central Instrumentation Facility Centre (CIFC)** at IIT(BHU) Varanasi, for providing essential facilities such as XRD, IR, HR-SEM, XPS, and AFM for sample characterization. Their support has been crucial in advancing my research.

I wish to express my heartfelt gratitude to **my family** for their unwavering love, care, and constant moral support. Their encouragement and steadfast belief in me have been a source of strength, empowering me to fulfil my responsibilities and reach this stage in my journey.

I am deeply thankful to all my juniors for their cooperation and the friendly environment they helped create throughout my research journey. My gratitude goes out to M.Sc. students **Gulshan Parashar, Pritesh Keshari, Tarul, Aakash Saxena, and Vikas Yadav**; IDD (B.Tech & M.Tech) students **Abhay Singh** and **Abhinav Pratap Singh Bais**; and Ph.D. students **Rashmi Yadav, Mithilesh Patel, and Saurav Yadav**. Their support and camaraderie have been invaluable throughout this period.

I would like to extend special thanks to my dear friends **Aayoosh Singh, Avanish Singh, Amit Singh, and Vikas Yadav**, whose unwavering support has been a constant source of strength, especially during challenging times. Their encouragement and friendship have meant the world to me.

I am sincerely grateful to the University Grants Commission (UGC) for their financial support throughout my research. Their assistance has been instrumental in enabling me to pursue and complete this work.

I am deeply grateful to my batchmates and friends— **Subrat Vishwakarma, Nitin Panwar, Ashish Kumar Yadav, Rajesh Kushwaha, Archana Pandey, Shikha Pandey, Yogita Rani, Priya,** and **Aswathi C.N.** —for their unwavering support, constructive discussion and invaluable advice.

To all my friends, relatives, and well-wishers, your encouragement and good wishes have been an invaluable source of strength throughout my journey. Though it would be impossible to name each of you individually, please know that I am deeply grateful for your support and belief in my success. Thank you, one and all.



**(Ankush Kumar Singh)**

---

---

## TABLE OF CONTENTS

---

---

CERTIFICATE.....	iii
DECLARATION BY THE CANDIDATE .....	iv
CERTIFICATE BY THE SUPERVISOR .....	iv
COPYRIGHT TRANSFER CERTIFICATE.....	v
ACKNOWLEDGEMENTS.....	vi
TABLE OF CONTENTS.....	x
LIST OF NOTATIONS, SYMBOLS AND ABBREVIATIONS .....	xiv
LIST OF FIGURES .....	xv
LIST OF TABLES.....	xx
PREFACE.....	xxi

### Chapter 1

#### *Introduction*

1.1. Brief History .....	2
1.2. Synthesis .....	5
1.3. Characterization of Graphitic Carbon Nitride .....	8
1.4. Modifications of Graphitic Carbon Nitride .....	9
1.4.1. Exfoliation:.....	10
1.4.2. Metal/Non-metal Doping: .....	11
1.4.3. Composites, Co-Polymerization and Heterojunction formation.....	12
1.5. Importance of Graphitic Carbon Nitride as Electrocatalyst.....	13
1.6. Immobilization of Electro-catalyst on Conductive Surfaces .....	15
1.6.1 Previously reported Immobilization strategies of gCN.....	15
1.6.2. Drop-cast method .....	19
1.6.3. Electrodeposition/Potentiodynamic Method.....	20
1.7. Electroanalytical Methods .....	21
1.7.1. Cyclic Voltammetry (CV).....	21
1.7.2. Square Wave Voltammetry .....	23
1.8. Targeted Parameters for investigating the electrocatalytic ability of modified gCN .....	24
1.9. Purpose and layout of the Thesis .....	25
1.10. References.....	26

## Chapter 2

### *Electrodeposition of Graphitic Carbon Nitride (gCN) & gCN.MnO<sub>2</sub> Composite for investigating Electrocatalytic Dopamine oxidation*

#### *First Part*

2.1.1. Introduction.....	51
2.1.2. Experimental.....	54
2.1.2.1. Materials.....	54
2.1.2.2. Synthesis of gCN.....	54
2.1.2.3 Characterization details.....	55
2.1.2.4. Electrochemical measurements.....	56
2.1.2.4.1 Electrodeposition of gCN, MnO <sub>2</sub> and gCN.MnO <sub>2</sub> composite.....	56
2.1.2.4.2 Electroanalytical technique and sample preparation.....	57
2.1.3. Results and Discussion.....	58
2.1.3.1 Physico-chemical characterization of the synthesised and ball-milled gCN ..	58
2.1.3.2 gCN Electrodeposition and In-Situ Decoration with MnO <sub>2</sub> Nanostructure: ...	62
2.1.3.2.1 Mechanistic Understanding.....	62
2.1.3.2.2 Protocol Optimization.....	65
2.1.3.2.3 Surface Characterization.....	66
2.1.3.3 Voltammetric Sensing of Dopamine as the Test Case.....	71
2.1.3.4 Stability and Reproducibility Studies.....	77
2.1.4. Conclusions.....	78
2.1.5. References:.....	79

#### *Second Part*

2.2 Introduction.....	93
2.2.2. Experimental.....	96
2.2.2.1. Materials.....	96
2.2.2.2. Synthesis of gCN.Mn <sub>x</sub> O <sub>y</sub> composites.....	96
2.2.2.3 Characterization details.....	97
2.2.2.4. Electrochemical measurements.....	97
2.2.2.4.1 Electrodeposition of gCN.MnO <sub>2</sub> composite.....	98
2.2.2.4.2 Electroanalytical technique and sample preparation.....	98
2.2.2.4.3 Real sample preparation and validation:.....	99
2.2.3. Result's and Discussion.....	100
2.2.3.1 Material Characterization: Examining the two gCN.Mn <sub>x</sub> O <sub>y</sub> composites.....	100
2.2.3.2 gCN.MnO <sub>2</sub> electrodeposition and unveiling the underlying mechanism:.....	106

2.2.3.2.1 Protocol Optimization .....	107
2.2.3.2.2 Surface Characterization .....	109
2.2.3.3 Analytical performance of modified electrode: Sensing of Dopamine.....	116
2.2.3.4 Real Sample Study .....	122
2.2.3.5 Reliability Studies .....	126
2.2.4. Conclusions.....	128
2.2.5. References:.....	129

### Chapter 3

#### *In-situ Growth of CuO Nanoflakes on Graphitic Carbon Nitride Sheets: An Electro-active Interface for Electrocatalytic Oxidation of Riboflavin.*

3.1 Introduction:.....	145
3.2. Experimental:.....	147
3.2.1 Chemicals .....	147
3.2.2 Synthesis Protocols .....	147
3.2.3 Characterization details .....	147
3.2.4 Electrochemical Set-up .....	148
3.2.5 Surface modified Electrode: Electrochemical synthesis of CuO nanoflakes decorated gCN.....	148
3.2.6 Electroanalytical Method .....	149
3.2.7 Real sample preparation: .....	149
3.3. Results and Discussion .....	151
3.3.1 Material Characterization: Examining the gCN.CuO composites .....	151
3.3.2 gCN.CuO electrodeposition and unveiling the underlying mechanism: .....	154
3.3.2.1 Protocol Optimization .....	155
3.3.2.2 Surface Characterization .....	157
3.3.3 Analytical performance of modified electrode: Sensing of Riboflavin .....	160
3.3.4 Interference Study .....	163
3.3.5 Real Sample Study .....	164
3.3.6 Reliability Studies .....	166
3.4. Conclusions.....	168
3.5. References:.....	169

### Chapter 4

#### *Electrodeposited Phosphorous Doped Graphitic Carbon Nitride for Electrocatalytic Oxidation of Tryptophan*

4.1. Introduction.....	179
4.2. Experimental:.....	182

4.2.1. Materials.....	182
4.2.2. Material Preparation.....	183
4.2.2.1. Synthesis of gCN.....	183
4.2.2.2. Synthesis of P-doped gCN.....	183
4.2.3 Characterization details.....	183
4.2.4. Electrochemical measurements.....	184
4.2.4.1 Electrodeposition of p-doped gCN Composite.....	184
4.2.4.2 Electroanalytical technique and sample preparation.....	185
4.3. Results and Discussion.....	188
4.3.1 Material Characterization: Examining the gCN and P-doped gCN composites.....	188
4.3.2 P-doped gCN electrodeposition and understanding the fundamental process:	192
4.3.2.1 Protocol Optimization.....	194
4.3.2.2 Surface Characterization.....	195
4.3.3. Assessment of the modified electrode's analytical performance: Tryptophan sensing.....	200
4.3.4 Interference Study.....	203
4.3.5 Real Sample Study.....	203
4.3.6 Stability, Repeatability and Reproducibility.....	206
4.4. Conclusions.....	208
4.5. References:.....	209

## **Chapter 5**

### *Conclusion, Summary and Future Outlook*

5.1. Major findings of each chapter.....	223
5.2. Comparative Evaluation:.....	228
5.2.1. Effect of substrate:.....	228
5.2.2. Comparison of modification strategies:.....	229
5.3. Future Perspective:.....	230
LIST OF PUBLICATIONS.....	232

---

---

## LIST OF NOTATIONS, SYMBOLS AND ABBREVIATIONS

---

---

<b>Notations</b>	<b>Abbreviations</b>
%	Percentage
<	Less than
>	More than
°	Degree
°C	Degree Celsius
©	Copyright
gCN	Graphitic Carbon Nitride
XRD	X-Ray Diffraction
FT-IR	Fourier transform infrared
XPS	X-ray photoelectron spectroscopy
UV	Ultraviolet
HR-SEM	High resolution scanning electron microscopy
EDX	Energy-dispersive X-ray
AFM	Atomic force microscopy
2D	Two-dimensional
CV	Cyclic voltammetry
SWV	Square wave voltammetry
ITO	Indium tin oxide
GCE	Glassy carbon electrode
SPE	Screen printed electrode
ECSA	Electrochemical surface area
LOD	Limit of detection
PB	Phosphate buffer
M	Molar
mM	Milli-molar
μM	Micro-molar
DI	Deionized water
DA	Dopamine
UA	Uric acid
AA	Ascorbic acid
HX	Hypoxanthine
MEL	Melatonin
TRP	Tryptophan
RF	Riboflavin



## LIST OF FIGURES

<b>Fig. No.</b>	<b>Figure Captions</b>	<b>Page No.</b>
<b>1.1</b>	Structure of "(a) Melamine (b) Melam (c) Melem (d) Melon prepared from the pyrolysis of mercury (II) thiocyanate as described by Liebig".	3
<b>1.2</b>	Structure of graphitic carbon nitride based on (a) s-triazine and (b) tri-s-triazine units.	4
<b>1.3</b>	Synthesis protocol of graphitic carbon nitride using different precursors.	6
<b>1.4</b>	Thermal polymerization of (a) cyanamide, (b) urea, and (c) thiourea to form graphitic carbon nitride.	7
<b>1.5</b>	Typical (a) XRD peaks, (b) FT-IR peaks, (c) C 1s, and (d) N 1s XPS spectra corresponding to gCN.	9
<b>1.6</b>	Figure representing the wide range of possible interactions for the fundamental unit of gCN.	10
<b>1.7</b>	Figure illustrating various possible sites for (A) non-metal and (B) metal doping.	12
<b>1.8</b>	Figure summarizing the various modification strategies commonly employed for tailoring gCN.	13
<b>1.9</b>	Doctor Blade method for coating of gCN slurry.	15
<b>1.10</b>	Different contact growth coating methods (a) Supramolecular Complex deposition. (b) Liquid-based growth and (c) Microwave-assisted condensation.	16
<b>1.11</b>	Different non-contact growth coating methods (a) Vapour deposition polymerization of precursor to gCN. (b) Microcontact-printing-assisted method of coating and (c) Thermal Vapour Condensation of precursor (Melamine) to gCN.	18
<b>1.12</b>	HR-SEM images of a drop casted gCN suspension on ITO surface showing different regions of non-uniform material distribution.	19
<b>1.13</b>	HR-SEM images of the gCN electrodeposited on ITO surface showing uniform coverage of the conducting surface.	21
<b>1.14</b>	Typical excitation signal in triangular wave form and the resulting cyclic voltammogram for a reversible redox process.	22
<b>1.15</b>	Typical excitation signal and observed response of square wave voltammetry.	23
<b>1.16</b>	SWV plot demonstrating increase in peak current and shift in peak potential as two important parameters for analysing the electrocatalytic activity.	25

<b>2.1.1</b>	(a) XRD pattern of melamine, ball-milled gCN, bulk gCN. (b) Comparative Raman spectra of bulk gCN and ball-milled gCN. Deconvoluted Raman spectra of (c) bulk gCN, and (d) ball-milled gCN.	59
<b>2.1.2</b>	FTIR spectra of bulk gCN and ball-milled gCN.	60
<b>2.1.3</b>	SEM images demonstrating surface morphology of (a,b) bulk gCN, and (c,d) ball-milled gCN.	61
<b>2.1.4</b>	(a-c) Cyclic voltammograms observed for electrodeposition of (a) gCN (b) MnO <sub>2</sub> and (c) gCN.MnO <sub>2</sub> composite. (d) Square wave voltammograms (e) bar diagram of current response observed using gCN.MnO <sub>2</sub> /ITO for 0.5 mM K <sub>3</sub> Fe(CN) <sub>6</sub> in KCl as a function of different number of electrodeposition scans. (f) Comparative square wave voltammograms recorded for 0.5 mM K <sub>3</sub> Fe(CN) <sub>6</sub> in KCl at Bare ITO (black), gCN/ITO (cyan), MnO <sub>2</sub> /ITO (olive) and MnO <sub>2</sub> .gCN/ITO (green).	64
<b>2.1.5</b>	HR-SEM images of (a) Bare ITO, (b) gCN/ITO, (c) MnO <sub>2</sub> /ITO, (d) gCN.MnO <sub>2</sub> /ITO. (e-h) represents the gCN.MnO <sub>2</sub> /ITO region used for elemental mapping of Mn, C, N and O, respectively. (j) Comparative AFM surface profile at 5 μm resolution for ITO and gCN.MnO <sub>2</sub> /ITO. 3D AFM surface profile of (k) ITO, and (l) gCN.MnO <sub>2</sub> /ITO.	67
<b>2.1.6</b>	(a,b) X-ray diffractogram of coated and uncoated ITO. X-ray photoelectron spectra of (c) ITO (full survey), (d) gCN.MnO <sub>2</sub> /ITO (full survey). (e) Mn 2p for gCN.MnO <sub>2</sub> /ITO, (f) deconvoluted N1s spectra for gCN.MnO <sub>2</sub> /ITO. Deconvoluted O1s spectra for (g) ITO, (h) gCN.MnO <sub>2</sub> /ITO. Deconvoluted C1s spectra for (i) ITO, and (j) gCN.MnO <sub>2</sub> /ITO. The light grey line in the XPS plots represents the raw data whereas the black dotted line represents the fitted data.	69
<b>2.1.7</b>	Cyclic voltammograms observed for 0.5 mM solution of K <sub>3</sub> [Fe(CN) <sub>6</sub> ] with varying scan rate from 10-150mV/s <sup>-1</sup> recorded using (a) ITO and (b) gCN.MnO <sub>2</sub> /ITO. Insets represents the corresponding I <sub>p</sub> vs. v <sup>1/2</sup> linear plots.	71
<b>2.1.8</b>	A comparative Square Wave Voltammograms of 150 μM of DA observed in PB 7.4 buffer at bare ITO (Saffron) and gCN.MnO <sub>2</sub> coated ITO (Green).	72
<b>2.1.9</b>	Concentration-dependent study: Square wave voltammogram recorded for 5 μM, 10 μM, 15 μM, 25 μM, 50 μM, 75 μM, 100 μM, 150 μM, 200 μM, 300 μM, 500 μM DA concentration using (a) bare ITO and (b) gCN.MnO <sub>2</sub> /ITO. Insets include the corresponding calibration plots for DA concentration from 5 μM to 300 μM.	73
<b>2.1.10</b>	The linear relation between I <sub>p</sub> Vs (f) and I <sub>p</sub> Vs (f) <sup>1/2</sup> recorded in 150 μM DA in pH-7.4 buffer with increasing frequencies from 5-50 Hz using bare ITO (a,b) and gCN.MnO <sub>2</sub> /ITO (c,d).	75
<b>2.1.11</b>	(a) Bar diagram representing the peak currents observed from square wave voltammograms recorded for fixed concentration of DA (150μM) in presence of 5-fold and 10-fold higher concentration of Uric acid, Melatonin and Dextrose using gCN.MnO <sub>2</sub> /ITO. Observed square wave voltammograms representing presence of DA in (b) pharmaceutical sample and (c) banana peel.	77
<b>2.1.12</b>	(a) Continuous 200 cycle voltammograms recorded in PB-7 using gCN.MnO <sub>2</sub> /ITO (b) SWV recorded in 0.5 mM solution of K <sub>3</sub> [Fe(CN) <sub>6</sub> ] using gCN.MnO <sub>2</sub> /ITO scaffolds at different time intervals.	78

2.2.1	(a) X-ray diffractogram of gCN, and gCN.Mn <sub>x</sub> O <sub>y</sub> composites. (b) FT-IR spectra of synthesized 9:1 and 7:3 gCN.Mn <sub>x</sub> O <sub>y</sub> composites. Comparative XPS plots of (c) Mn 2p, (d) O 1s, (e) N 1s and (f) C 1s corresponding to 9:1 and 7:3 gCN.Mn <sub>x</sub> O <sub>y</sub> composites.	103
2.2.2	Scanning electron microscopy images of (a,b) 9:1 gCN.Mn <sub>x</sub> O <sub>y</sub> and (c,d) 7:3 gCN.Mn <sub>x</sub> O <sub>y</sub> composite.	104
2.2.3	EDX of (a) 9:1 gCN.Mn <sub>x</sub> O <sub>y</sub> (b) 7:3 gCN.Mn <sub>x</sub> O <sub>y</sub> material. (c-d) Elemental mapping of 7:3 gCN.Mn <sub>x</sub> O <sub>y</sub> showing uniform distribution of C, O, Mn and N over the scanned area.	105
2.2.4	(a,b) Comparative first (a) and second (b) cyclic voltammograms observed during electrodeposition of 9:1 and 7:3 gCN.Mn <sub>x</sub> O <sub>y</sub> composite. Full electrodeposition cyclic voltammograms observed for (c) 9:1 gCN.Mn <sub>x</sub> O <sub>y</sub> (d) 7:3 gCN.Mn <sub>x</sub> O <sub>y</sub> . (e) Square wave voltammograms observed for Bare ITO, gCN ITO, 9:1 gCN.Mn <sub>x</sub> O <sub>y</sub>  ITO and 7:3 gCN.Mn <sub>x</sub> O <sub>y</sub>  ITO for 0.5 mM K <sub>3</sub> [Fe(CN) <sub>6</sub> ] in KCl. (f) Square wave voltammograms observed for 0.5 mM K <sub>3</sub> [Fe(CN) <sub>6</sub> ] in KCl as a function of different number of electrodeposition scans using 7:3 gCN.MnO <sub>2</sub>  ITO.	108
2.2.5	Square wave voltammograms observed for 0.5 mM K <sub>3</sub> [Fe(CN) <sub>6</sub> ] in KCl as a function of scan rate employed for the electrodeposition of gCN.MnO <sub>2</sub> using 7:3 gCN.Mn <sub>x</sub> O <sub>y</sub> .	109
2.2.6	HR-SEM images of (a) Bare ITO at 1 μm, (b) gCN.MnO <sub>2</sub> coated ITO at 1 μm, (c,d) The scanned area and corresponding elemental mapping of gCN.MnO <sub>2</sub>  ITO.	110
2.2.7	(a) X-ray diffraction patterns observed for ITO and gCN.MnO <sub>2</sub>  ITO. XPS (b) Full survey, (c) Mn 2p, (d) O 1s, (e) N 1s and (f) C 1s spectra of gCN.MnO <sub>2</sub>  ITO	112
2.2.8	AFM 3D profiles observed for the (a,c) ITO and (b,d) gCN.MnO <sub>2</sub>  ITO. Cyclic Voltammograms recorded at different scan rates ranging from 10 mV/s to 200 mV/s using (e) Bare, and (f) gCN.MnO <sub>2</sub>  SPE in 0.5 mM K <sub>3</sub> [Fe(CN) <sub>6</sub> ] solution.	113
2.2.9	Linear regression plot of current vs (scan rate(v)) <sup>1/2</sup> for (a) bare SPE (b) gCN.MnO <sub>2</sub>  SPE recorded for various scan rate in K <sub>3</sub> [Fe(CN) <sub>6</sub> ] solution.	114
2.2.10	A comparative (a) Cyclic Voltammograms (b and c) Square Wave Voltammograms of 0.5 mM of K <sub>3</sub> [Fe(CN) <sub>6</sub> ] recorded using bare SPE, gCN.MnO <sub>2</sub>  SPE and SPE modified by drop-casting 10 μL of 7:3 gCN.Mn <sub>x</sub> O <sub>y</sub> suspension. (d) Square Wave Voltammograms of 100 μM of DA observed in PB 7.4 buffer at bare SPE and gCN.MnO <sub>2</sub> coated SPE. SWV observed using (e) bare SPE at different concentrations ranging from 30 μM to 500 μM and (f) using modified SPE at different concentrations ranging from 50 nM to 50 μM.	118
2.2.11	Linear regression plot of current vs f and current vs f <sup>1/2</sup> for (a) bare SPE (b) gCN.MnO <sub>2</sub>  SPE recorded using 100 μM DA in a pH 7.4 buffer solution.	121
2.2.12	(a) Interference Study: Square wave voltammogram representing the variation in the DA (20 μM) peak currents recorded in presence of different concentration of Ascorbic Acid (AA), Uric Acid (UA), Tryptophan (TRP) and Melatonin (MEL) using gCN.MnO <sub>2</sub>  SPE. (b-e) Real sample analysis: square wave voltammograms representing the presence of DA in (b) commercial DA hydrochloride injection, (c) human blood serum, (d) urine, and (e) human saliva.	123

<b>2.2.13</b>	(a) 100 consecutive cyclic voltammograms recorded in Phosphate Buffer (PB 7.4) using gCN.MnO <sub>2</sub>  SPE. (b) First fifty square wave voltammograms and (c) respective variation in current percentages as observed for 0.5 mM K <sub>3</sub> [Fe(CN) <sub>6</sub> ] using single gCN.MnO <sub>2</sub>  SPE. (d) Square wave voltammograms recorded for 0.5 mM K <sub>3</sub> [Fe(CN) <sub>6</sub> ] using 5 different gCN.MnO <sub>2</sub>  SPE.	127
<b>3.1</b>	(a) Comparative XRD pattern, (b) Comparative FT-IR spectra of graphitic carbon nitride and its composite with CuO. (c) SEM image of synthesized graphitic carbon nitride (d) SEM images of graphitic carbon nitride-CuO composite.	152
<b>3.2</b>	The surface elemental mapping of the as-synthesized gCN.CuO material.	153
<b>3.3</b>	(a,b) Continuous CV curves recorded during electrodeposition of graphitic carbon nitride-CuO composite; Comparative SWV curves recorded using (c) bare GCE, gCN GCE, and gCN.CuO GCE; (d) gCN.CuO GCE relating the variation in peak current of 500 μM potassium ferricyanide solution in response to surface modification and the number of electrodeposition scans.	155
<b>3.4</b>	SWV curves of 500 μM potassium ferricyanide solution recorded using unmodified, drop-casted, and electrodeposited gCN.CuO GCE	157
<b>3.5</b>	XPS spectrum of (a) Cu 2p; (b) O 1s; and (c) C 1s for gCN.CuO GCE. HR-SEM image of (d) Bare GCE, and (e-g) gCN.CuO modified GCE (gCN.CuNF GCE).	158
<b>3.6</b>	Cyclic voltammograms recorded in 500 μM potassium ferricyanide using (a) unmodified GCE and (b) gCN.CuNF GCE as a function of different scan rate.	160
<b>3.7</b>	Comparative SWV curves recorded for 100 μM RF using (a) Bare GCE and gCN GCE; (b) Bare GCE and gCN.CuNF GCE. Concentration-dependent SWV curves were recorded in RF concentration ranging from 25 nM to 100 μM using (c) bare GCE and (d) gCN.CuNF GCE.	161
<b>3.8</b>	Calibration plot relating the peak current with the RF concentration recorded using (a) bare GCE, and (b) gCN.CuNF GCE.	162
<b>3.9</b>	(a) Interference Study: SWV curves recorded in presence of 10 to 100 fold B <sub>12</sub> , AA UA, HX for RF using gCN.CuNF GCE. (b-f) Real sample analysis: SWV demonstrating detection of RF in (b) Becosules Syrup, (c) Zincovit Tablet, (d) Almond, (e) Curd, and (f) Hershey's Shake.	164
<b>3.10</b>	(a) 200 consecutive CV curves recorded in blank (pH 7, PB buffer) using gCN.CuNF GCE; SWV responses recorded in 500 μM potassium ferricyanide solution representing variation in current: (b) for first 100 measurements (in percentage) (c) first 30 days (d) using three different GCE for modification.	167
<b>4.1</b>	(a) XRD comparison of as synthesized gCN and all different P doped gCN composite. (b) FT-IR comparison of as synthesized gCN and all different P doped gCN. HR-SEM image of (c) gCN, (d) P-gCN-02, (e) P-gCN-05, and (f) P-gCN-10.	189
<b>4.2</b>	(a) XPS full survey comparison of as synthesized gCN and P-gCN-05 (b) High resolution deconvoluted P 2p spectra of P-gCN-05 (c) High resolution deconvoluted C 1s spectra for gCN. (d) High resolution deconvoluted C 1s spectra compare for P-gCN-05. (e) High resolution deconvoluted N 1s spectra for gCN. (f) High resolution deconvoluted N 1s spectra compare for P-gCN-05.	191

<b>4.3</b>	Cyclic voltammograms observed during electrodeposition of (a) gCN and (b) P-gCN-05. (c) Square wave voltammograms observed for 0.5 mM $K_3[Fe(CN)_6]$ in KCl using bare GCE, gCN   GCE, P-gCN-02   GCE, P-gCN-05   GCE and P-gCN-10   GCE. Square wave voltammograms observed for 0.5 mM $K_3[Fe(CN)_6]$ in KCl using P-gCN-05   GCE as a function of (d) different suspension concentrations of P-gCN-05, (e) Increasing numbers of electrodeposition cycles, (f) surface modification method i.e. drop casted P-gCN-05   GCE, and electrodeposited P-gCN-05   GCE.	193
<b>4.4</b>	X-ray photoelectron spectra of (a) Full survey for P-gCN-05   GCE (b) Deconvoluted spectra of C 1s (c) Deconvoluted spectra of N 1s, and (d) Deconvoluted spectra of P 2p for P-gCN-05   GCE. HR-SEM image of (e) Electrodeposited gCN   GCE and (f) Electrodeposited P-gCN-05   GCE.	196
<b>4.5</b>	SEM Images of Bare GCE, gCN   GCE and P-gCN   GCE with corresponding elemental mapping of gCN   GCE and P-gCN-05   GCE.	197
<b>4.6</b>	AFM profiles observed for the (a, b) Bare GCE and (b, d) P-gCN-05   GCE.	198
<b>4.7</b>	Cyclic Voltammograms recorded at different scan rates ranging from 5 mV/s to 200 mV/s using (a) Bare GCE, and (b) P-gCN-05   GCE in 0.5 mM $K_3[Fe(CN)_6]$ solution.	199
<b>4.8</b>	Comparative (a) Cyclic voltammograms (b) Square wave voltammograms recorded for 100 $\mu$ M TRP using Bare GCE and P-gCN-05   GCE. Concentration study and corresponding correlation graph observed for (c) Bare GCE (d) P-gCN-05   GCE.	201
<b>4.9</b>	Interference Study: (a) Square wave voltammogram using 25 $\mu$ M of TRP with 1,2- and 3-times higher concentrations of interferents. Real sample analysis: square wave voltammograms representing the presence of TRP in (b) Almond, (c) Pista, (d) Oats, (e) Chickpea, (f) Kidney beans, (g) Turmeric powder, (h) Carrot, (i) Pumpkin, (j) Egg white, (k) TRP nutritional supplement capsule, (l) Urine, and (m) Blood serum.	204
<b>4.10</b>	(a) 200 consecutive cyclic voltammograms recorded in Phosphate Buffer (PB 7.4) using P-gCN-05   GCE. (b) First fifty square wave voltammograms as observed for 0.5 mM $K_3[Fe(CN)_6]$ using single P-gCN-05   GCE. (c) Long term durability current response of 0.5 mM $K_3[Fe(CN)_6]$ for different day using P-gCN-05   GCE. (d) Square wave voltammograms recorded for 0.5 mM $K_3[Fe(CN)_6]$ using 3 different P-gCN-05   GCE.	207
<b>5.1</b>	Graphical representation to summarize Chapter 2 (Part 1).	224
<b>5.2</b>	Graphical representation to summarize Chapter 2 (Part 2).	225
<b>5.3</b>	Graphical representation to summarize Chapter 3.	226
<b>5.4</b>	Graphical representation to summarize Chapter 4.	227
<b>5.5</b>	Comparative study of gCN electrodeposition and drop-casting on (a) ITO (b) GCE (c) SPE.	229
<b>5.6</b>	Comparative study of gCN and its composites on the glassy carbon electrode.	229



---



---

## LIST OF TABLES

---



---

Table No.	Titles	Page No.
1.1	Brief Historical progress of gCN	4
2.1.1	Comparison of the proposed gCN.MnO <sub>2</sub> /ITO scaffold with the reported DA electrochemical sensors developed using gCN, metal oxides and related surface modifiers	74
2.1.2	Determination of DA content in commercially available IV injection.	77
2.2.1	Comparison of the reported electrochemical sensors developed for DA estimation using gCN, metal oxides, and similar surface modifications with the proposed gCN.MnO <sub>2</sub>  SPE scaffold.	120
2.2.2	Quantification of DA in real samples using gCN.MnO <sub>2</sub>  SPE.	125
3.1	Comparative performance analysis of the proposed sensor with the recently reported voltammetric sensors for RF estimation	163
3.2	Quantification of RF in real samples using gCN.CuNF GCE	165
4.1	A comparison of published electrochemical sensors established for TRP measurement employing gCN, metal oxides, and similar surface modifications with the proposed P-gCN-05   GCE scaffold.	202
4.2	Quantification of TRP in different real samples using P-gCN-05   GCE	205-06



---

---

## PREFACE

---

---

Graphitic carbon nitride (gCN), a metal-free, two-dimensional (2D) material, has garnered significant interest due to its high chemical/mechanical stability, tunable molecular structure, catalytic efficacy, environmental sustainability, and easy synthesis. From a structural perspective, gCN features a structure close to graphene with a honeycomb configuration with s-triazine or tri-s-triazine aromatic heterocycle as the fundamental unit. The  $sp^2$  hybridization of carbon and nitrogen atoms in the aromatic ring of tri-s-triazine gCN establishes a delocalized  $\pi$ -conjugated system with C-N layers linked by weak van der Waals forces. Because of the  $\pi$ -conjugated system, abundant C and N sites, and tunable band gap, gCN swiftly emerged as a prominent green catalyst in the domain of photo-catalysis, including  $CO_2$  capture and reduction, photocatalytic degradation, and photocatalytic water splitting reactions. Nonetheless, the application of gCN in the electrochemical field has not been explored much. Its restricted use is due to its low electrical conductivity, leading to sluggish charge transfer. Another problem is its bulk structure, which is mainly obtained from the thermal pyrolysis of N and C-rich precursors like melamine. The bulk structure offers a limited surface area and poor mass transfer, offering a suppressed electrochemical response. Its low dispersibility in most of the solvents and high N content are a few other problems that make bulk gCN an ineffective choice for electrochemical processes. However, the ease of surface functionalization and its ability to interact with various metals offer tremendous venues for tailoring its composition and structure to tune the physicochemical properties of the bulk gCN as per the electrochemist's need.

Along the same line, this thesis is focused on overcoming the aforementioned drawbacks associated with gCN and utilizing it as an electrocatalyst by tailoring its morphology,

structure, and composition. The thesis revolves around synthesizing the bulk gCN, opting for unconventional exfoliation strategies, and making composites with metal and non-metal components. Therefore, the thesis is divided into **five chapters**:

The **first chapter** comprehensively introduces gCN, covering its brief history, structural features, advantages, various preparation methods, and limitations regarding electrocatalytic activity. Furthermore, the first chapter addresses the various methods of catalyst immobilization on conductive electrodes, along with their associated drawbacks. At the conclusion of the first chapter, the rationale for selecting the electrodeposition protocol for gCN immobilization on the electrode was discussed, along with a detailed explanation of the methods employed for electrodeposition and catalytic activity testing, specifically Cyclic Voltammetry and Square Wave Voltammetry.

The **second chapter** of the thesis consists of two distinct sections. The first part addresses the synthesis, characterization, and electrodeposition of bulk and ball-milled gCN. This chapter features the step-by-step mechanistic understanding of the electrodeposition and the protocol optimization in terms of scan rate, number of scans, and material. The electrodeposition was confirmed through in-depth spectroscopic, microscopic, and electrochemical tools. The chapter further presents the incorporation of MnO<sub>2</sub> to achieve a synergistic enhancement of electrocatalytic activity. The electrodeposition of gCN.MnO<sub>2</sub> was carried out using two strategies. Firstly, gCN.Mn<sub>x</sub>O<sub>y</sub> was synthesized and then the electrodeposition was carried out. In the second approach, the in-situ formation and electrodeposition of gCN.MnO<sub>2</sub> on more viable, screen-printed electrode was targeted. The electrocatalytic activity of the modified surfaces were characterized by comparing the enhancement in the peak current (sensitivity) and the shift in the peak

potential for an ideal redox probe  $K_3[Fe(CN)_6]$  and for the dopamine electro-oxidation, a widely recognized neurotransmitter.

In the **third chapter**, the gCN.CuO composite was synthesized and characterized. The CuO is specifically selected to enhance the electrochemical performance of gCN by means of the interaction between the  $\pi$ - $\pi$  electron cloud and with high spin density N of polymeric gCN structure and the vacant d orbitals of Cu(II). The synthesized composite was electrodeposited on a glassy carbon electrode and subsequently characterized. Following the electrodeposition, the gCN.CuO composite exhibited a distinctly altered morphology characterized by nano-flakes. The electrochemical performance of the modified and unmodified surface was then compared for the investigation of the electro-oxidation of an ideal redox probe  $K_3[Fe(CN)_6]$ . Lately, due to the complexing ability of CuO with Riboflavin, the modified electrode was used for the electroanalysis of Riboflavin.

After modifying the gCN with metals, the **fourth chapter** addresses tuning the electrocatalytic activity of gCN with phosphorus doping. gCN with three distinct P-doping percentages were synthesized and thoroughly characterized. The electrocatalytic activity of the P-doped gCN modified surface was studied using an ideal redox probe  $K_3[Fe(CN)_6]$ . The best-performing material was then employed to study the interfacial electrochemistry of tryptophan for qualitative and quantitative analysis.

The **fifth chapter** of this thesis summarizes the research comparing the electrocatalytic activity of all the mentioned composites, draws conclusions, and discusses future perspectives related to this work.